

# Eliashberg theory for anisotropic couplings: a renormalization-group approach

R. Roldán<sup>1,2</sup> and Shan-Wen Tsai<sup>2</sup>

<sup>1</sup>*Instituto de Ciencia de Materiales de Madrid, CSIC, Cantoblanco, E-28049 Madrid, Spain*

<sup>2</sup>*Department of Physics and Astronomy, University of California, Riverside, CA 92521, USA*

(Dated: May 26, 2019)

We study the problem of superconductivity mediated by anisotropic electron-boson couplings. Starting from a circular Fermi surface for non-interacting electrons, electron-electron interactions and anisotropic electron-boson couplings are treated with a renormalization-group method that takes into account retardation effects. We find analytical solutions for the flow equations and derive generalized Eliashberg equations from which generalized McMillan and Allen-Dynes expressions for  $T_c$  are obtained. Numerical solutions for a few illustrative examples show how the vertices depend on the frequencies of the electrons for parameters ranging from the weak to the strong coupling limits. The form of this dependence is different for different symmetry channels and provides insight on the validity of two-step renormalization-group methods.

Eliashberg theory[1, 2] of superconductivity was originally formulated to describe phonon-mediated  $s$ -wave superconductors. Since then, it has been applied to other pairing symmetries[3, 4, 5], especially  $d$ -wave, mediated by anisotropic boson couplings, such as spin fluctuations[6]. Eliashberg equations are written in terms of the reduced Coulomb repulsion  $\mu^*$  (Anderson-Morel potential[7]) and the Eliashberg function  $\alpha^2 F(\omega)$ , which defines  $\lambda = 2 \int_0^\infty \alpha^2 F(\omega) d\omega / \omega$ . These microscopic parameters can be obtained from tunneling experiment[8, 9].

The renormalization-group (RG) method for interacting electrons[10] has been extended to also include electron-boson (el-bos) couplings[11]. Using the non-interacting electron Fermi surface (FS) as the starting point, microscopic interactions are treated within one-loop RG. The interactions are parameterized by the on-site Coulomb repulsion  $u_0$ , el-bos coupling  $g$  and Einstein frequency  $\omega_E$ . In this case  $\lambda = 2N(0)g^2/\omega_E$ . Solution of the RG flow equations shows that there is a superconducting (SC) instability, and the formal solution at this point was shown to be exactly the Eliashberg equations at  $T = T_c$ [10]. The Anderson-Morel potential emerges naturally from the RG equations as  $\mu^* = u_0/(1 + \ell_E u_0)$ , where  $\ell_E = \ln(\Lambda_0/\omega_E)$  and  $\Lambda_0$  is the initial energy bandwidth. Eliashberg theory assumes Migdal's theorem[12] holds, and, in the RG approach, this can be understood in terms of a large- $N$  expansion[11]. The value of  $T_c$ , and the McMillan[13] and Allen-Dynes[14, 15] analytical expressions can be obtained from the RG solution. This RG method has since been applied to Holstein-Hubbard chains and ladders [16], and also to two-dimensional (2D) systems at half-filling[17]. There has also been work in which the RG flows are extended into the SC phase[18].

Here we consider the most general case of anisotropic coupling of electrons to bosonic modes, containing a combination of many symmetry channels. The RG flow equations for the BCS (particle-particle) vertices can be decomposed in angular momentum channels. However, the kernel of these equations contains corrections

to the quasiparticle weight, which is related to the imaginary part of the electron self-energy  $\Sigma''(\omega, \mathbf{k})$  and is momentum-dependent, with contributions from all the components of the el-bos coupling.  $\Sigma''(\omega, \mathbf{k})$  gets renormalized because the effective el-el interaction is retarded. We study the breakdown of the Fermi liquid (FL) state towards SC by analytical and numerical solution of the flow equations, and also by mapping the instability conditions into Eliashberg equations at  $T_c$ . The numerical solution provides information about how the frequency dependence of the vertices change with the RG flow, and we find interesting behavior that depends on the symmetry of the channel, as we go from weak to strong coupling limit. A set of generalized Eliashberg equations and corresponding McMillan and Allen-Dynes expressions for  $T_c$  are derived from the RG flow equations for this case.

*1. Renormalization-group analysis.* The el-bos coupling leads to a retarded effective el-el interaction  $\tilde{u}(4, 3, 2, 1) = u(4, 3, 2, 1) - 2g(1, 3)g(2, 4)D(1-3)$ , where the phonon propagator is  $D(q) = \omega_q / (\omega^2 + \omega_q^2)$  with  $q = (\omega, \mathbf{q})$ ,  $1 = (\omega_1, \mathbf{k}_1)$ , and so forth. Particles 1 and 2 are incoming and scatter into 3 and 4, respectively. Spin indices are omitted here and we focus on processes involving particles with opposite spins. The processes involving particles with same spins can be obtained from these due to SU(2) symmetry[19]. We consider a 2D square lattice at fillings significantly smaller than one half, so that the FS is almost circular. For such FS, the only vertex that flows under RG at one-loop is the BCS vertex ( $k_1 = -k_2, k_3 = -k_4$ ), whereas the forward channel ( $k_1 = k_3, k_2 = k_4$ ), which does not get renormalized, contributes to the electron self-energy [10]. The RG equation for the BCS vertex at one-loop is given by[11]:

$$\frac{d}{d\ell} \tilde{u}(1, 3, \ell) = - \int_{-\infty}^{\infty} \frac{d\omega}{\pi} \int_0^{2\pi} \frac{d\theta}{2\pi} \frac{\Lambda_\ell \tilde{u}(1, \omega, \theta, \ell) \tilde{u}(\omega, \theta, 3, \ell)}{\Lambda_\ell^2 + Z_\ell^2(\omega, \theta) \omega^2} \quad (1)$$

where here  $1 \equiv (\omega_1, \theta_1)$  and  $3 \equiv (\omega_3, \theta_3)$ . The vertices are labeled according to the angle around the FS since the dependence on the radial part of the momentum is irrelevant[10]. To solve this differential equation

we decompose the pairing potential in terms of the irreducible representation of the space group of the underlying lattice —  $D_4$  for the case of a 2D square lattice. The irreducible representations of the  $D_4$  space group contains four singlets:  $A_1$  and  $A_2$  for conventional and unconventional  $s$ -wave channels,  $B_1$  for  $d_{x^2-y^2}$ -channel and  $B_2$  for  $d_{xy}$ -channel; and one triplet:  $E$ , corresponding to  $p$ -wave symmetry, with degenerate eigenvalues for the two channels  $p_x$  and  $p_y$ . So we can write  $\tilde{u}(i, j, \ell) = \sum_{\gamma} \sum_{m,n} u_{mn}^{\gamma}(\omega_i, \omega_j, \ell) f_{mn}^{\gamma}(\theta_i, \theta_j)$ , where  $\gamma$  labels the representations of the group and  $f_{mn}^{\gamma}(\theta_i, \theta_j) = \phi_m^{\gamma}(\theta_i) \phi_n^{\gamma}(\theta_j)$ , with  $\phi_m^{\gamma}(\theta)$  the corresponding basis functions, and  $m$  ranging from 0 to  $\infty$ .

Using the orthogonality and completeness of the  $\phi$ -basis and discretizing the frequency integral into a sum, we can rewrite the flow equation (1) as a *tensor* equation:

$$\frac{d}{d\ell} (\hat{u}_{nm}^{\gamma})_{\beta}^{\alpha}(\ell) = - \sum_{\delta=-N}^N \sum_{i,j=0}^M (\hat{u}_{ni}^{\gamma})_{\delta}^{\alpha}(\ell) \left( \hat{K}_{ij}^{\gamma} \right)_{\delta}^{\alpha}(\ell) (\hat{u}_{jm}^{\gamma})_{\beta}^{\delta}(\ell), \quad (2)$$

where we have imposed an upper limit to the harmonic index  $n < M$ , and to the frequency sum. In this equation,  $(\hat{u}_{nm}^{\gamma})_{\beta}^{\alpha}(\ell) = \int d\theta_{\alpha} \int d\theta_{\beta} \tilde{u}(\alpha, \beta, \ell) \phi_n^{\gamma}(\theta_{\alpha}) \phi_m^{\gamma}(\theta_{\beta})$ , and  $\left( \hat{K}_{ij}^{\gamma} \right)_{\beta}^{\alpha}(l) = K_{ij}^{\gamma}(\omega_{\alpha}, \ell) \delta_{\beta}^{\alpha}$ , with

$$K_{ij}^{\gamma}(\omega_{\alpha}, \ell) = \int_0^{2\pi} d\theta [\Lambda_{\ell}/(\Lambda_{\ell}^2 + Z_{\ell}^2(\omega, \theta) \omega^2)] \phi_i^{\gamma}(\theta) \phi_j^{\gamma}(\theta). \quad (3)$$

Equivalently, (2) can be written in compact form as a  $(2N+1)M \times (2N+1)M$  matrix equation:  $d\mathbf{U}^{\gamma}/d\ell = -\mathbf{U}^{\gamma} \cdot \mathbf{K}^{\gamma} \cdot \mathbf{U}^{\gamma}$ , where the matrix index  $j$  is related to the frequency ( $\alpha$ ) and harmonic ( $n$ ) indices by  $\alpha = \text{int}(\frac{j-1}{M}) + 1$ , and  $n = j - \text{Mint}(\frac{j-1}{M})$ , where  $\text{int}()$  denotes the integer part. There is one vertex flow equation for each channel  $\gamma$ . With RG flow equations for the vertices in matrix form, it is now simple to write the exact solution[11]:

$$\mathbf{U}^{\gamma}(\ell) = [\mathbf{1} + \mathbf{U}^{\gamma}(0) \cdot \mathbf{P}^{\gamma}(\ell)]^{-1} \cdot \mathbf{U}^{\gamma}(0), \quad (4)$$

where  $\mathbf{P}^{\gamma}(\ell) \equiv \int_0^{\ell} d\ell' \mathbf{K}^{\gamma}(\ell')$ . There is an instability of the FL state when  $\mathbf{U}^{\gamma}(\ell_c) \rightarrow \infty$  at  $\ell = \ell_c$ . This condition is reached when  $\det[\mathbf{1} + \mathbf{U}^{\gamma}(0) \cdot \mathbf{P}^{\gamma}(\ell_c)] = 0$ , which is equivalent to solving the eigenvalue equation

$$[\mathbf{1} + \mathbf{U}^{\gamma}(0) \cdot \mathbf{P}^{\gamma}(\ell_c)] \cdot \mathbf{v}^{\gamma} = 0. \quad (5)$$

The kernel  $\mathbf{K}^{\gamma}(\ell)$  that appears in the vertex flow equations is given by (3) and contains self-energy corrections. The imaginary part of the self-energy is related to the quasiparticle-weight by  $\Sigma_{\ell}''(\omega, \theta) = [1 - Z_{\ell}(\omega, \theta)]\omega$ . It is renormalized by the bare forward vertices, and the flow equation for  $Z_{\ell}(\omega, \theta)$  can be integrated to give:

$$Z_{\ell}(\omega_{\alpha}, \theta_{\alpha}) = 1 + \frac{2}{\pi \omega_{\alpha}} \int_{\Lambda_{\ell}}^{\Lambda_0} d\Lambda_{\ell'} \int_{\theta_{\beta} \omega_{\beta}} \frac{N(0) \tilde{u}_0(\alpha, \beta) Z_{\ell'}(\omega_{\beta}, \theta_{\beta}) \omega_{\beta}}{\Lambda_{\ell'}^2 + Z_{\ell'}^2(\omega_{\beta}, \theta_{\beta}) \omega_{\beta}^2} \quad (6)$$

where  $\tilde{u}_0(\alpha, \beta) = u_0 - 2g^2(\theta_{\alpha}, \theta_{\beta})D(\omega_{\alpha} - \omega_{\beta})$ , and  $N_0$  is the electron density of states at the Fermi level. The self-energy is angle-dependent and it appears as a term in the denominator of  $\mathbf{K}^{\gamma}(\ell)$ . Therefore, while only the  $\gamma$ -component  $\mathbf{K}^{\gamma}(\ell)$  of the kernel contribute to a given channel  $\gamma$ , all  $\gamma$ -components of the microscopic el-bos coupling contribute to  $\mathbf{K}^{\gamma}(\ell)$ .

*2. Eliashberg equations.* At finite temperatures,  $T = T_c$  is the scale when the SC instability occurs and FL breaks down. Since the instability is approached by decreasing the temperature, the integration over  $\Lambda$  in Eq.(5,6) can be taken all the way to zero. In the finite  $T$  formalism  $Z$  also depends on  $T$  and an expression similar to (5) gives the condition for the instability from which  $T_c$  can be obtained. Writing the integrals over frequencies as Matsubara sums, (5) and (6) give the set of generalized Eliashberg equations at  $T_c$ :

$$v^{\gamma}(\omega_n, \theta) = \pi T_c \sum_{\omega_m} \frac{1}{|\omega_m|} \int_{\theta'} \Gamma_{\theta, \theta'}^{\gamma}(\omega_n - \omega_m) \frac{v^{\gamma}(\omega_m, \theta')}{Z(\omega_m, \theta', T_c)} \quad (7)$$

$$Z(\omega_n, \theta, T_c) = 1 + \pi T_c \sum_{\omega_m} \bar{\Gamma}_{\theta}(\omega_n - \omega_m) \quad (8)$$

where

$$\Gamma_{\theta, \theta'}^{\gamma}(\omega_{\alpha} - \omega_{\beta}) \equiv - \int_{\theta_{\alpha}, \theta_{\beta}} N(0) \tilde{u}_0(\alpha, \beta) \eta^{\gamma}(\theta_{\alpha}, \theta) \eta^{\gamma}(\theta_{\beta}, \theta') \quad (9)$$

$$\bar{\Gamma}_{\theta_{\alpha}}(\omega_{\alpha} - \omega_{\beta}) \equiv - \int_{\theta_{\beta}} \frac{N(0)}{2\pi} \tilde{u}_0(\alpha, \beta) \quad (10)$$

with  $\eta^{\gamma}(\theta_{\beta}, \theta) = \sum_{p=1}^{\infty} \phi_p^{\gamma}(\theta_{\beta}) \phi_p^{\gamma}(\theta)$ . Note that  $u_0$  in the definition above does not contribute in the expression for  $Z$  because it does not depend on frequency and the Matsubara sum for this term vanishes. The quantities  $\Gamma_{\theta, \theta'}^{\gamma}(\omega_{\alpha} - \omega_{\beta})$  and  $\bar{\Gamma}_{\theta}(\omega_{\alpha} - \omega_{\beta})$  are related. Consider first the special case in which  $g(\theta_{\alpha}, \theta_{\beta})$  is separable, that is, has the form  $g(\theta_{\alpha}, \theta_{\beta}) = f(\theta_{\alpha})f(\theta_{\beta})$ , and set  $u_0 = 0$  for now. Then  $\Gamma_{\theta, \theta'}^{\gamma}$  will also be separable:  $\Gamma_{\theta, \theta'}^{\gamma}(\omega_{\alpha} - \omega_{\beta}) = \Gamma_{\theta}^{\gamma}(\omega_{\alpha} - \omega_{\beta}) \Gamma_{\theta'}^{\gamma}(\omega_{\alpha} - \omega_{\beta})$ , where  $\Gamma_{\theta}^{\gamma}(\omega_{\alpha} - \omega_{\beta}) \equiv \int_{\theta_{\alpha}} f^2(\theta_{\alpha}) \sqrt{2N(0)D(\omega_{\alpha} - \omega_{\beta})} \eta^{\gamma}(\theta_{\alpha}, \theta)$ . We will also have:  $\bar{\Gamma}_{\theta}(\omega_{\alpha} - \omega_{\beta}) = \frac{1}{2\pi} \int_{\theta'} \bar{\Gamma}_{\theta}(\omega_{\alpha} - \omega_{\beta}) \bar{\Gamma}_{\theta'}(\omega_{\alpha} - \omega_{\beta})$ , where  $\bar{\Gamma}_{\theta}(\omega_{\alpha} - \omega_{\beta}) \equiv \sum_{\gamma} \Gamma_{\theta}^{\gamma}(\omega_{\alpha} - \omega_{\beta})$ . In the general case, since  $g(\theta_{\alpha}, \theta_{\beta}) = g(\theta_{\beta}, \theta_{\alpha})$ , we can always write  $g(\theta_{\alpha}, \theta_{\beta}) = \sum_i f_i(\theta_{\alpha})f_i(\theta_{\beta})$  so that:

$$\begin{aligned} \Gamma_{\theta, \theta'}^{\gamma}(\omega_{\alpha} - \omega_{\beta}) &= \sum_i \Gamma_{i\theta}^{\gamma}(\omega_{\alpha} - \omega_{\beta}) \Gamma_{i\theta'}^{\gamma}(\omega_{\alpha} - \omega_{\beta}) \\ \bar{\Gamma}_{\theta}(\omega_{\alpha} - \omega_{\beta}) &= \frac{1}{2\pi} \sum_i \int_{\theta'} \bar{\Gamma}_{i\theta}(\omega_{\alpha} - \omega_{\beta}) \bar{\Gamma}_{i\theta'}(\omega_{\alpha} - \omega_{\beta}) \end{aligned} \quad (11)$$

The equations derived here reduce to those given by earlier treatment of Eliashberg theory for anisotropic el-bos interaction done by Daams and Carbotte[3] if we consider a single separable channel, say,  $\gamma = 2$  and  $n = 0$ .

From the generalized Eliashberg equations, one can obtain the value of  $T_c$  in terms of the microscopic parameters. For the most general case, analytical expressions

for  $T_c$  are quite involved. However, if for a given channel  $\gamma$  the gap is dominated by one component  $q$  such that the SC gap can be written as  $\Delta_\gamma(\theta) = \Delta_0 \phi_q^\gamma(\theta)$ , then the corresponding McMillan's expression[13] for  $T_c$  becomes:

$$T_c^\gamma \approx \omega_E \exp \left\{ \frac{Z_\gamma}{\mu^* \delta_{\gamma 1} - \lambda_\gamma} \right\} \quad (12)$$

where  $\delta_{\gamma 1}$  restricts the contribution of  $\mu^*$  to the channel  $\gamma=1$  ( $u_0$  only has first harmonic of  $s$ -wave component),  $Z_\gamma^{-1} = \int_\theta \phi_q^\gamma(\theta) / [1 + \bar{\lambda}(\theta)]$  and

$$\lambda_\gamma = Z_\gamma \sum_p \int_{\theta_\alpha, \theta_\beta, \theta} \frac{\lambda(\theta_\alpha, \theta_\beta) \phi_p^\gamma(\theta_\alpha) \eta^\gamma(\theta_\beta, \theta) \phi_q^\gamma(\theta)}{1 + \bar{\lambda}(\theta)} ,$$

with  $\lambda(\theta_\alpha, \theta_\beta) \equiv \frac{2N(0)g^2(\theta_\alpha, \theta_\beta)}{\omega_E}$ ,  $\bar{\lambda}(\theta) \equiv \frac{1}{2\pi} \int_{\theta'} \lambda(\theta, \theta')$ . The corresponding Allen-Dynes expression is  $T_c \approx \sqrt{\bar{\lambda}_\gamma} \omega_E$ , where  $\bar{\lambda}_\gamma \equiv \sum_p \int_{\theta_\alpha, \theta_\beta, \theta} \lambda(\theta_\alpha, \theta_\beta) \phi_p^\gamma(\theta_\alpha) \eta^\gamma(\theta_\beta, \theta) \phi_q^\gamma(\theta)$ .

*3. Specific cases.* The method used allows for an easy numerical calculation of the critical temperature  $T_c$  (and the zero temperature gap  $\Delta_0$ ) from the microscopic parameters  $u_0$ ,  $\lambda$  and  $\omega_E$ . Eq.(4) gives the RG evolution of all the vertices and can be evaluated at different RG steps  $\ell$ . To find the instability, one can also simply calculate the quantity  $\det[1 + \mathbf{U}^\gamma(0) \cdot \mathbf{P}^\gamma(\ell)]$  and see when it approaches zero.

Here we study el-bos couplings with different angular dependences and strengths going from the weak to the strong regimes. For  $g(\theta, \theta') = g_0 \cos(\theta - \theta')$ , only channels  $\gamma = 1, 2$  contribute, corresponding to  $s$ - and  $d_{x^2-y^2}$ -symmetry. Fig. (1) shows the evolution of  $\mathbf{U}^\gamma(\ell)$  with  $\ell$  for the  $s$ -channel. Each panel represents the  $(2N + 1)M \times (2N + 1)M$  metric  $\mathbf{U}^s(\ell)$  at a given RG step  $\ell$ . The matrix elements corresponding to small frequencies are at the center of the panels. The three left panels of Fig. (1) show the evolution for a case in the weak coupling regime ( $\lambda \equiv 2N_0 g_0^2 / \omega_E = 0.4$ ). The first one shows the initial condition. The third one shows the vertices right before the instability happens: the most divergent couplings are the ones with frequencies below the Einstein frequency,  $|\omega_\alpha|, |\omega_\beta| < \omega_E$ . In this case simple two-step RG can be applied. The three panels on the right of Fig. (1) represents the evolution of the couplings for the strong el-bos interaction regime ( $\lambda = 4$ ). In this case, the most divergent couplings are the ones with frequencies below an energy scale  $W_c > \omega_E$ . As expected, these results are similar to that of [20] where the el-bos coupling was taken to be isotropic.

Fig. (2) shows the SC vertices for the  $d_{x^2-y^2}$ -channel. Again, the left hand side corresponds to the weak coupling regime which has a similar initial condition. Close to the instability, the couplings  $u^d(\omega_\alpha, \omega_\beta, \ell_c)$  that first diverge correspond to a region of frequencies centered around  $\omega = 0$  and with a star shape. The left hand side of Fig. (2) represents the flow, in the strong coupling

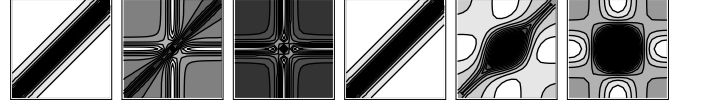


FIG. 1: Plots of the  $(2N + 1)M \times (2N + 1)M$  matrix  $\mathbf{U}^\gamma(\ell)$  at different RG scales  $\ell$  for the  $s$ -channel ( $\gamma = 1$ ). Here, for the first harmonic in the expansion ( $M = 1$ ), the number of frequency divisions is 21 ( $N = 10$ ) and  $\Lambda_0 = 100$ ,  $\omega_E = 10$ ,  $u_0 = 0.1$ . The three panels on the left correspond to  $\lambda = 0.4$  (weak coupling) and the three on the right correspond to  $\lambda = 4$  (strong coupling).

regime, from the initial condition to the critical RG step  $\ell_c$  where the most divergent couplings, as in the  $s$ -wave case, are those with frequencies below  $W_c$ . In Fig. (3) we

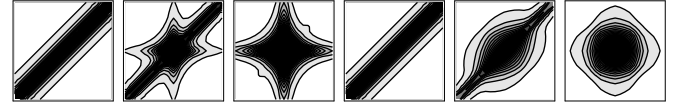


FIG. 2: Same as Fig.[1] but for the  $d_{x^2-y^2}$ -channel ( $\gamma = 2$ ). The three panels on the left are for weak coupling ( $\lambda = 0.4$ ) and the ones on the right are for the strong coupling regime ( $\lambda = 4$ ).

show how the density plots of the matrix  $\mathbf{U}^s(\ell_c)$  change from weak to strong el-bos coupling for the on-site repulsion  $u_0 = 2$ . Here we can see more clearly how the energy scale separating high and low energy physics moves from the Einstein frequency  $\omega_E$  in the weak coupling range, to the critical cutoff  $W_c$  in the strong coupling regime. The scale  $W_c$  can be associated with the  $T = 0$  SC gap  $\Delta_0$ , or with the critical temperature  $T_c$  of SC phase in the finite temperature formalism[11, 20]. Fig. (3) also illustrates the breakdown of the two-step RG. In this approximation, the vertex is chosen to be just the electron-electron part for frequencies above the Einstein frequency, and to have some constant contribution from the boson modes for frequencies below  $\omega_E$  [21]. This approximation works in the weak coupling limit, where the most divergent couplings are that with frequencies below  $\omega_E$ . But for a large  $\lambda$  ( $\lambda \gg 1$ ) this behavior breaks down and the scale for the divergent central region is of order  $W_c > \omega_E$ .

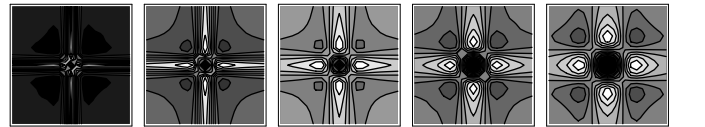


FIG. 3: Coupling matrix  $\mathbf{U}^s(\ell_c)$  at the instability point for the  $s$ -channel from weak to strong coupling for  $u_0 = 2$ . Panels correspond to  $\lambda = 1.2, 2, 4, 6, 10$ .

Similarly, Fig. (4) shows the couplings  $\mathbf{U}^d(\ell_c)$  in the  $d_{x^2-y^2}$ -channel, for weak to strong el-bos coupling regimes. We obtain the star-like structure in the weak

coupling ( $\lambda = 0.01$ ) that evolves towards a more symmetrical behavior in the intermediate to strong coupling ( $\lambda = 4$ ). For very strong couplings ( $\lambda = 6, 10$ ) we again obtain the most divergent matrix elements to be confined in a small region around  $\omega = 0$ . More analytical study is required for an understanding of these patterns. Fig. (5) shows the energy scale  $W_c$  as a function of the

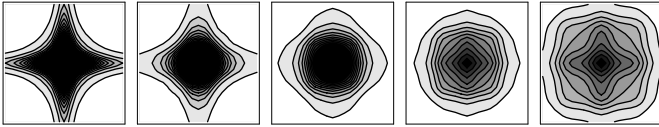


FIG. 4: Coupling matrix  $\mathbf{U}^d(\ell_c)$  at the instability point for the  $d_{x^2-y^2}$ -channel from weak to strong coupling. Panels correspond to  $\lambda = 0.01, 2, 4, 6, 10$ .

strength of el-bos coupling at fixed  $\omega_E$ . The two channels that contribute,  $s$  and  $d$ , are represented. The behavior of  $W_c$  follow the Mc-Millan and Allen-Dynes forms in the corresponding regimes of small or large  $\lambda$ . The inset of Fig. (5) shows the phase diagram of the system where, in the finite- $T$  case, we have a FL phase that breaks down towards  $d_{x^2-y^2}$ -SC in the weak to intermediate coupling range, and to  $s$ -wave SC for the intermediate to strong coupling regime. The larger the on-site electronic repulsion  $u_0$ , the larger the el-bos coupling crossover  $\lambda_{s-d}$  that separates the  $s$ -SC region from the  $d_{x^2-y^2}$ -SC region will be. This is expected since an isotropic  $u_0$  only suppresses the  $s$ -wave channel without affecting the other channels. For  $u_0 = 0$  there is SC only in the  $s$ -channel.

We have also studied the case of a el-bos coupling  $g(\theta, \theta') = g_0 \cos(\theta/2) \cos(\theta'/2)$ , where  $s$ - and the  $p$ -channels are present. For  $u_0 = 0.1$ , FL state is unstable

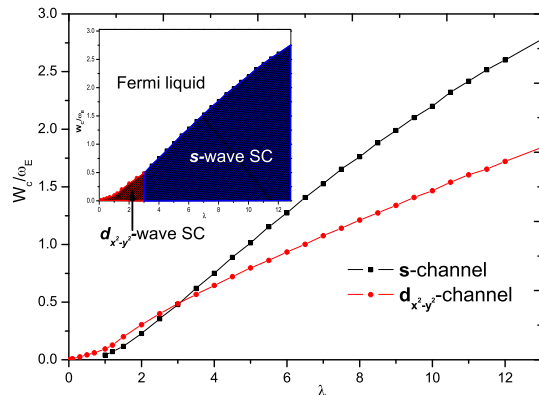


FIG. 5: Critical cutoff  $W_c$  versus  $\lambda$  for the  $s$ -channel (black squares) and the  $d_{x^2-y^2}$ -channel (red circles). The value of the parameters used are  $\Lambda_0 = 100$ ,  $\omega_E = 10$  and  $u_0 = 2.0$ . The inset represents the phase diagram.

towards  $p$ -wave SC for  $0 < \lambda \lesssim 0.7$ , and towards  $s$ -wave

SC for larger couplings,  $\lambda \gtrsim 0.7$ . For the  $p$ -channel, the frequency dependence of the coupling matrix also show the star-shaped structure at weak el-bos couplings.

*Conclusions.* In this work we study the pairing instabilities of the FL state due to the presence of anisotropic boson exchange couplings. We use a RG approach where the starting point is the non-interacting FS and interactions are treated at one-loop level. Retardation effects are taken fully into account by keeping the frequency dependence of the interaction vertices and the self-energy. We consider here a circular FS for which the RG flow equations can be solved analytically. At the instability, the RG solution gives generalized Eliashberg equations at  $T_c$  from which Mc-Millan- and Allen-Dynes-type equations are obtained. Numerical evaluation of the flows are instructive in determining the range of important frequencies in different regimes and for different symmetry channels. In particular,  $d$ - and  $p$ -wave pairing channels show a richer dependence of the couplings on frequencies.

Funding from MCyT (Spain) through grant FIS2005-05478-C02-01 is acknowledged. We appreciate useful conversations with A. H. Castro Neto, F. D. Kliromos and M. P. López Sancho.

---

- [1] G. M. Eliashberg, *Zh. Exp. Teor. Fiz.* **38**, 966 (1960).
- [2] J. P. Carbotte, *Rev. Mod. Phys.* **62**, 1027 (1990).
- [3] J. M. Daams and J. P. Carbotte, *J. of Low Temp. Phys.* **43**, 263 (1981).
- [4] A. J. Millis, S. Sachdev, and C. M. Varma, *Phys. Rev. B* **37**, 4975 (1988).
- [5] A. V. Balatsky and J.-X. Zhu, *Phys. Rev. B* **74**, 094517 (2006).
- [6] A. J. Millis, *Phys. Rev. B* **45**, 13047 (1992).
- [7] P. Morel and P. W. Anderson, *Phys. Rev.* **125**, 1263 (1962).
- [8] W. L. McMillan and J. M. Rowell, *Phys. Rev. Lett.* **14**, 108 (1965).
- [9] D. J. Scalapino, in *Superconductivity*, Vol. 1, edited by R. D. Parks (Dekker, New York, 1969).
- [10] R. Shankar, *Rev. Mod. Phys.* **66**, 129 (1994).
- [11] S.-W. Tsai *et al.*, *Phys. Rev. B* **72**, 054531 (2005).
- [12] A. B. Migdal, *Zh. Eksp. Teor. Fiz.* **34**, 1438 (1958).
- [13] W. L. McMillan, *Phys. Rev.* **167**, 331 (1968).
- [14] C. R. Leavens and J. P. Carbotte, *Can. J. Phys.* **49**, 724 (1971).
- [15] P. B. Allen and R. C. Dynes, *Phys. Rev. B* **12**, 905 (1975).
- [16] K.-M. Tam *et al.* (2006), cond-mat/0603055, cond-mat/0607700.
- [17] F. D. Kliromos and S.-W. Tsai, *Phys. Rev. B* **74**, 205109 (2006).
- [18] C. Honerkamp and M. Salmhofer, *Prog. Theor. Phys.* **113**, 1145 (2005).
- [19] D. Zanchi and H. J. Schulz, *Phys. Rev. B* **61**, 13609 (2000).
- [20] S.-W. Tsai *et al.*, *Phil. Mag.* **86**, 2631 (2006).
- [21] J. Polchinski, *Nucl. Phys. B* **422**, 617 (1994).